

# Charge State Sensor for Thermal Energy Storages Based on Phase Change Slurries

Jorrit Wronski<sup>1</sup>, Clemens Pollerberg<sup>1\*</sup>, Carel W. Windt<sup>2</sup>, Li Huang<sup>1</sup>,  
Christian Dötsch<sup>1</sup> and Armin Knels<sup>3</sup>

<sup>1</sup> Fraunhofer Institute UMSICHT, Osterfelder Str. 3, 46047 Oberhausen, Germany

<sup>2</sup> Forschungszentrum Jülich, ICG-III: Phytosphäre, Leo-Brand-Str. 1, 52428 Jülich, Germany

<sup>3</sup> RWTH Aachen, E.ON Energy Research Center - EBC, Mathieustr. 6, 52074 Aachen, Germany

\* Corresponding Author, clemens.pollerberg@umsicht.fraunhofer.de

## Abstract

The present paper describes different techniques that can be used to determine the charge state of a phase change slurry. The functional fluid used is a surfactant stabilised paraffin-in-water dispersion containing different amounts of phase change material. Density, nuclear magnetic resonance (NMR) relaxometric properties and ultrasonic velocity are measured and evaluated. Results from heating the dispersion at a constant gradient of  $0.25 \text{ Kmin}^{-1}$  from  $5 \text{ °C}$  to  $35 \text{ °C}$  corresponds to the peak melting rate identified by differential scanning calorimetry. The employed sensors are part of a test rig made from standard components and data is acquired from three experimental runs. Thermal expansion of the paraffin is derived from measured data and is linked to its state of aggregation. The  $T_2$  NMR relaxation spectrum of protons within the fluid is used to estimate the amount of solid-, melting- and liquid material inside the wax droplets. Though theoretically suitable, the speed of ultrasound can hardly be determined with the used standard equipment. Its application is limited to dilute dispersions.

## 1. Introduction

Energy demand and generation do not occur simultaneously. Especially the performance of renewable energy systems suffers from this mismatch. Energy transport and storage technology therefore is the key to an extended and efficient use of renewable energy sources. A large share of domestic and industrial thermal energy applications operate at temperatures relatively close to ambient conditions. The main storage and transport agent for such low temperature heat and cold supply systems is water. Following the above, the specific heat of water and the maximum allowed temperature range limit the overall ability to store energy.

Utilising a phase change material (PCM) enhances the performance of supply networks by enabling the exploitation of the latent heat of fusion. Since this phase transition enthalpy is received and released at the melting point of a given substance, its total heat capacity increases considerably at the corresponding temperature. The oldest PCM of relevance to engineering application is ice. Hence, the operating temperature of latent heat energy storage systems had to be close to  $0 \text{ °C}$ . To overcome this limitation, current latent heat energy storage systems employ two additional groups of substances as storage agent, hydrates and saturated hydrocarbons. By blending the latter, paraffin can be tailored to match the exact needs of a certain application in terms of temperature. Additional challenges in the

design of systems with paraffin-based phase change material arise from the properties of the solid state. It is not easy to handle and its low heat conductivity complicates the realisation of high heat transfer rates. As described in [1], dispersing PCM in a continuous phase, which remains liquid during the phase transition of the PCM, improves heat transfer and assures fluid-like behaviour. Fraunhofer UMSICHT conducts research on surfactant-stabilised paraffin-in-water dispersions (P/W dispersions) as heat transfer and storage medium. Despite the fact that there is an increased viscosity, [2] states that a functional dispersion might lead to electricity savings by reducing the pumping effort. Different hydrocarbon blends and mass fractions account for specific applications, most of which are connected to air conditioning, but also space heating with low temperature heat is discussed.

## 2. Motivation

As shown in Fig. 1, the maximum heat flow occurs within a rather narrow temperature range. This holds true for the upper curve, heating, as well as the lower one, which is recorded during cooling. Uncertainties of temperature measurements result in erroneous calculations of the energy content.

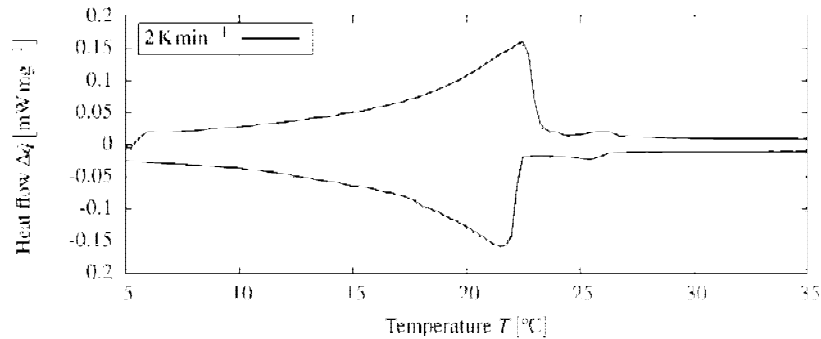


Fig. 1. DSC measurement of a phase change slurry sample scanned at  $2 \text{ K min}^{-1}$ .

Furthermore, temperature-based charge state estimations always take thermodynamic equilibrium for granted. Depending on the kind of paraffin, the droplet size distribution and the heating and cooling rates, such equilibrium cannot be assured for most applications. Supercooling effects are inevitable and decrease the point of fusion up to six Kelvin below the melting point for dispersions. Blending in small amounts of hydrocarbons with a much higher melting point reduces supercooling, however it cannot be eliminated completely. Thus, temperature alone is not suitable as reference value to monitor the exact difference in energy content of forward and backward flow. Following the approach taken in [3] and [4] for slurry ice, the amount of solidified material inside a PCS directly relates to its latent heat charge state. Mass flow  $\dot{m}$ , temperature  $T$ , paraffin content  $x_{PCM}$ , solid fraction  $x_{sol}$ , heat of fusion  $h_{fus}$  and the single-phase heat capacities of water  $c_{p,H_2O}$ , frozen  $c_{p,sol}$  and molten  $c_{p,liq}$  PCM define this enthalpy. Assuming that the specific heat capacities and the heat of fusion remain constant, continuous measurement of the other quantities is desirable. As mass flow and temperature sensors are conventional instruments, online solid content determination is the challenge that needs to be met. This paper describes the experimental setup and the results of density, nuclear magnetic resonance (NMR) relaxometry and ultrasound measurements recorded during phase transition cycles of the PCS.

Density is investigated since there is a step-like discontinuity at the phase transition in the common exponential thermal expansion for most substances. While melting, paraffin density decreases by a remarkably high magnitude of 10–15 %. This high value even encouraged the authors of [5] to design actuators based on this effect. NMR relaxometry is a well-established technique to study the properties and composition of complex mixtures. The basic principle behind NMR relaxometry is that the NMR signal of protons in different physicochemical environments decays with different speeds. For a detailed introduction, please see [6]. The most useful parameter in basic relaxometry is the transverse relaxation rate, also called  $T_2$  relaxation rate. Different proton mobility leads to a range of  $T_2$  relaxation times, from the microsecond scale in solids, up to a few seconds in liquids. Here, NMR relaxometry is employed to study and quantify the melting and freezing of paraffin droplets in a PCS solution. Since sound propagation depends on density and compressibility, the influence of the inner phase's state of aggregation on the overall value is even larger than for density alone. In most solids, the speed of sound can be considered as constant, whereas it decreases with rising temperature in common liquids. Actual values for solid and liquid paraffin appear in [7] and [8]. The decrease of 30 % at the melting point of paraffin is about twice the magnitude of the density changes.

### 3. Experiments and Procedure

Building a test rig that holds all the equipment needed to acquire data for all three quantities enables simultaneous measurements and assures the comparability of the data. Fig. 2 shows a sketch of piping and instruments of the apparatus used for this purpose; it is not true to scale.

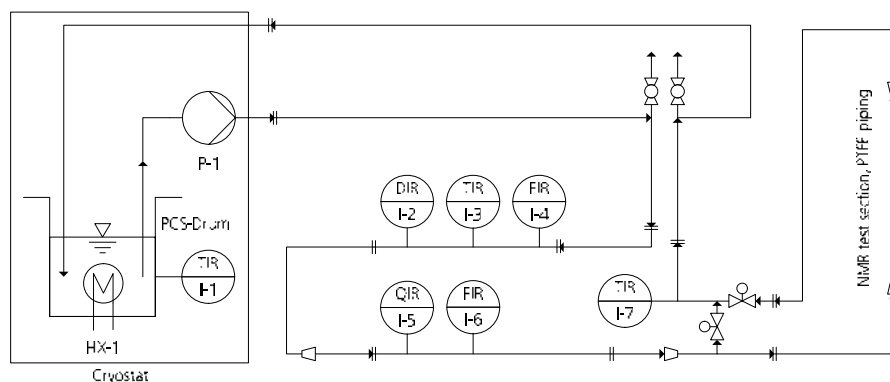


Fig. 2. Test rig used for experiments.

Below, the path of the PCS on its way from the storage tank through the test rig and back is illustrated. The parts inside the box on the left hand side all belong to a thermostat (Huber Kältemaschinenbau, Offenburg, Germany). A standard PT-100 temperature sensor is mounted at this thermostat. TIR-I-1 measures temperature inside the vessel that is connected to pump P-1. Temperature controlled PCS leaves the thermostat and runs through a standard hose. Reaching the first hose connector, the fluid enters the stainless steel construction and travels down a DN 15 pipe to the first measurement device. The densitometer Promass80F (Endress+Hauser, Ratingen, Germany) records density DIR-I-2, temperature TIR-I-3 and mass flow FIR-I-4. The following u-shaped pipe with a 180 ° elbow and a flaring from DN 15 to DN 50 allows a flow profile to develop before the flow enters the ultrasound measurement unit. Analysis is carried out by a SONO 3300, which basically is a piece of pipe equipped with

four transducers, and the corresponding data processing device FUS060 (both Siemens Flow Instruments, Nordborg, Denmark). The latter provides sound velocity QIR-I-5 as a current signal and volumetric flow FIR-I-6 as a frequency. Downstream from there, the pipe diameter decreases back to DN 15 before the NMR section. Inside the NMR magnet itself, a proton-free polytetrafluoroethylene (PTFE) pipe is used. The PTFE section is mounted into the circuit by means of screw joints, which connect the PTFE part to flexible standard tubing. In order to avoid outflow effects in the NMR measurements, the flow in the section that leads into the NMR magnet needs to be stopped whenever an NMR scan is acquired. For this purpose, two solenoid valves are used to open and close the NMR and shortcut section of the circuit in an alternating fashion.

For the NMR measurements, a custom-built portable 24.42 MHz Halbach magnet with a 3 cm central bore as described in [9] is employed. It is fitted with a solenoid radio frequency (rf) coil with 11 windings and an inner diameter of 10 mm. The magnet is paired with a Kea 2 spectrometer, equipped with a built-in 100 W amplifier (Magritek, Wellington, New Zealand). Two types of measurements are done in an alternating fashion. First, a free induction decay (FID) is acquired with a spectral width (SW) of 1 MHz, 512 complex points and 8 averages. Subsequently, a Carr, Purcell, Meiboom, Gill (CPMG) measurement is done with an SW of 250 KHz, 2000 echoes, echo time 250  $\mu$ s, 16 complex points per echo and 16 averages. The  $T_2$  relaxation spectrum is subsequently obtained by means of the Non-Negative Least Squares (NNLS) fitting procedure in the Prospa data evaluation package (Magritek, Wellington, New Zealand).

Further downstream, the fluid enters steel piping again and passes the last temperature measurement TIR-I-7, which is realised as a passive PT-100 without a transducer. Running through another hose, the P/W dispersion ends up in the vessel of the thermostat again. In order to avoid peculiarities caused by supercooling during solidification, all data presented here was recorded during the heating phase of subsequent melting and solidification cycles. One experimental run consists of four parts. In total, this investigation consists of three runs with the same temperature programme. First, the system is heated up to 60 °C in approximately 20 min so that all paraffin, including the nucleating agent, melts. Accumulations, which might have formed over some time of inactivity, melt and the homogeneity of the system is restored. Afterwards, the dispersion is cooled to 5 °C in 90 min and kept at that temperature for another 30 min. This abets the solidification of most droplets and accounts for the thermal mass of the test rig. The actual measurement consists of a temperature ramp from 5 °C to 35 °C. The data acquisition system records density, sound velocity, mass flow and temperature whilst the thermostat continuously heats the fluid. With the chosen slope of 0.25 K min<sup>-1</sup>, one measurement cycle takes approximately two hours. Switching the solenoid valves on the right hand side of Fig. 2 every 10 s enables the complete replacement of the fluid inside the test section as well as the completion of the actual NMR scan.

By increasing the temperature of the liquid inside the test rig over a trajectory of 30 °C, the temperature of the rf coil is increased as well. Since the amplitude of the NMR signal will decrease with increasing rf coil temperature, this effect will have to be compensated for. For this purpose the first 10 points of the FID measurement, comprising signal from all protons in the solid, liquid and melting fractions in the PCS mixture, are averaged and used as a 100 % reference value for each temperature step. These reference values are subsequently used to correct for the temperature effect on the amplitudes in the  $T_2$  relaxation spectra.

## 4. Results and Discussion

### 4.1. Density

The data acquisition system operates at a sampling rate of approximately 1 Hz. Converting these time-based readings into temperature related data gives a meaningful illustration of the phase change. All samples within  $\pm 0.25$  °C are averaged and the result is mapped to the centre of this interval. Since the results for pure water are in good agreement with reference data provided in [10], the whole measurement chain works reliably. Assuming that nucleating agent and surfactant (average density  $960 \text{ kg m}^{-3}$ ) make up 2 wt.%, the paraffin density can be extracted. A comparison with theoretical densities of wholly liquid and wholly solid paraffin leads to Fig. 3 and enables the calculation of the solid content. The curves for single-phase paraffin are obtained from

$$\rho_{liq} = 750 \text{ kg m}^{-3} \exp(1 \times 10^{-3} \text{ K}^{-1} (70 \text{ °C} - T)) \quad (1)$$

$$\rho_{sol} = 870 \text{ kg m}^{-3} \exp(1 \times 10^{-3} \text{ K}^{-1} (15 \text{ °C} - T)). \quad (2)$$

Both resemble the standard thermal equation formula. Whereupon the parameters are drawn from the data sheet of the paraffin RT 20 (Rubitherm Technologies, Berlin, Germany). The thermal expansion coefficient is assumed to be constant and equal for liquid and solid material. According to [11], values for pure saturated hydrocarbons vary noticeably, exempli gratia  $1.56 \times 10^{-3} \text{ K}^{-1}$  for pentane and  $0.89 \times 10^{-3} \text{ K}^{-1}$  for tetradecane. Following [12], the value of  $1 \times 10^{-3} \text{ K}^{-1}$  is a feasible approximation for paraffin waxes outside the phase change area.

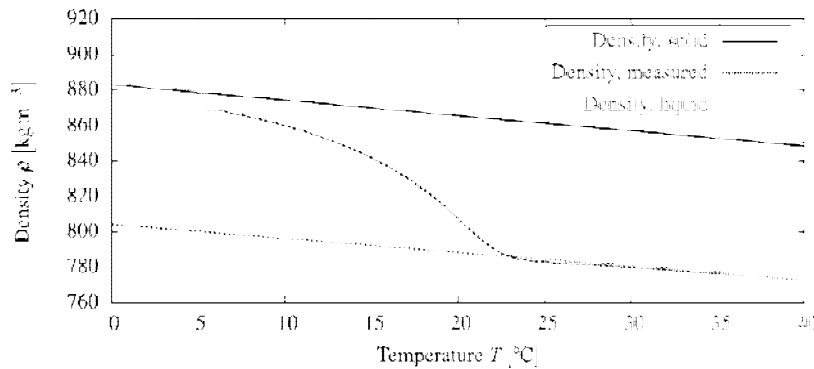


Fig. 3. Calculated paraffin droplet density, theoretical values for single phase material.

Since density is a volume-based property, the deviation of the measured data from the solid and liquid state gives the volume fraction of solid paraffin, which is converted into the mass-based solid fraction  $x_{sol}$ . As can be seen in Fig. 3, the phase transition process starts already below 5 °C and gains momentum with increasing temperature. From 23 °C on, the measured density follows the liquid density curve. Hence, the phase change is completed and all droplets are molten.

### 4.2. NMR Relaxometry

Since constant temperature is assumed for one set of CPMG scans, their outcome is drawn as horizontal isothermal lines in Fig. 4. Amplitude is depicted by the colour intensity; at small values, contour lines are used to enhance the visibility. In the CPMG measurement, the experimental parameters were chosen such that solids, with  $T_2$  relaxation times in the microsecond range, remain invisible. Fractions

with  $T_2$  relaxation times between 1 and 200 ms can be assigned to melting paraffin on the outside of paraffin globules with a solid core, or to pockets of molten paraffin still trapped in a solid matrix. When completely molten, the signal from paraffin globules can no longer be distinguished from that of the surrounding water. At this point all fractions are observed to possess a  $T_2$  of around 900 ms.

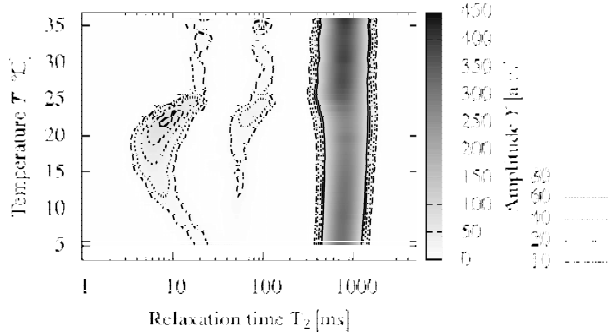


Fig. 4.  $T_2$  relaxation spectra of the PCS during a temperature run. The indicated amplitudes correlate with proton density.

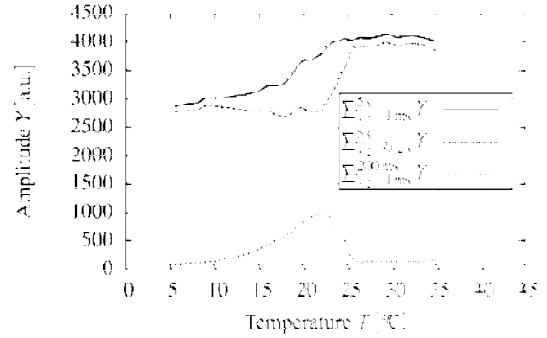


Fig. 5. Plot of the cumulative amplitudes of the  $T_2$  fractions. Dashed line: liquid fraction, dotted line: melting fraction, black line: all signal.

As can be seen in Fig. 5, most paraffin melts between 20 °C and 25 °C and the overall signal increases steadily up to this temperature. Assuming that all paraffin is solid at 5 °C, at the beginning of the temperature run, and liquid at 35 °C at the end of the experiment, the difference between the signal at 5 and 35 °C provides a quantitative measure for the amount of paraffin in the PCS. The amplitudes shown relate directly to proton density. Because the proton densities for paraffin and water are different, the different amplitudes cannot be used to calculate the relative volume ratios directly. For this, an additional calibration step would be needed.

### 4.3. Ultrasound Velocity

Although flow meters based on ultrasonic techniques are common equipment, measuring the speed of sound inside multiphase media is a challenging task. Caused by different heat capacities of dispersed and continuous phase, the temperature wave, which accompanies sound propagation, changes its amplitude at interfaces. Heat flow occurs and affects the volume expansion at the boundary layer, which creates a source of scattering. Additional scattering appears due to density differences, inertia forces cause a relative movement of bubbles, droplets and particles inside a dispersion. Such a movement compresses and expands the continuous phase around the moving volume, these pressure variations also contribute to the overall scattering as explained in [13]. The present P/W dispersion attenuates sound very efficiently. PCS with a paraffin content of more than 17 wt.% could not be investigated. Referring to Fig. 6, readings get unstable and signal strength as well as quality drop below acceptable values. Data for Fig. 6 is acquired from series of experiments with dispersion, which is watered down manually. In order to gather more reliable ultrasound data, Fraunhofer UMSICHT is in contact with a supplier for ultrasonic equipment. However, the speed of sound measured in dilute dispersions decreases with temperature. Theoretical binary mixtures of water with solid and liquid paraffin exhibit an increasing sound velocity. Thus, the paraffin inside the sample undergoes a phase transition and ultrasonic velocimetry is capable of following it.

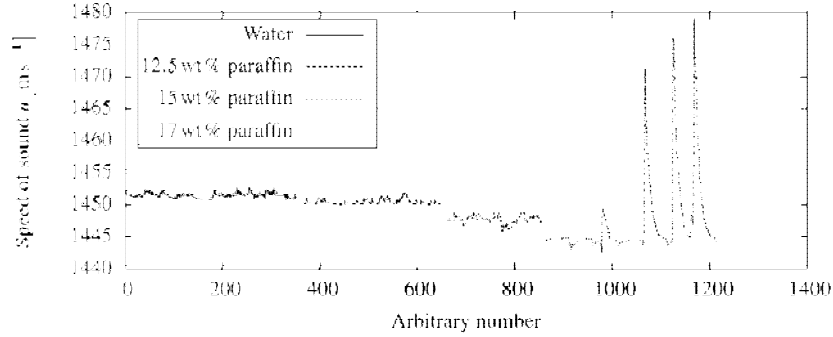


Fig. 6. Speed of sound in a P/W dispersion with different weight fractions of paraffin.

## 5. Conclusion

All measurement techniques are able to spot the phase transition inside a PCS. During the melting of the inner phase of the dispersion, density and NMR relaxation investigations give stable and reproducible results for a PCS with 21 wt.% paraffin in a test rig made from standard industry equipment. The ultrasound equipment at hand cannot determine the speed of sound. Additional experiments exhibited an unacceptable attenuation for fluids with more than 17 wt.% paraffin. Dispersion density can be mapped to the solid paraffin content  $x_{sol}$  in a straightforward manner, see (3). However, results still need to be verified by measuring the thermal expansion within the phase transition range and for single-phase paraffin. Despite needing an additional calibration to quantitatively determine the overall amount of solid material, NMR relaxometry delivered promising results and is considered a valuable technique for characterising a PCS. Computation of the solid content is carried out by

$$x_{sol,density} = \frac{\phi_{sol}\rho_{sol}}{(1-\phi_{sol})\rho_{liq} + \phi_{sol}\rho_{sol}} \quad \text{with} \quad \phi_{sol} = \frac{\rho - \rho_{liq}}{\rho_{sol} - \rho_{liq}} \quad \text{and} \quad (3)$$

$$x_{sol,NMR} = \frac{\max(f) - f}{\max(f) - \min(f)} \quad \text{with} \quad f = \sum_{T_2=1ms}^{5s} Y(T_2, T). \quad (4)$$

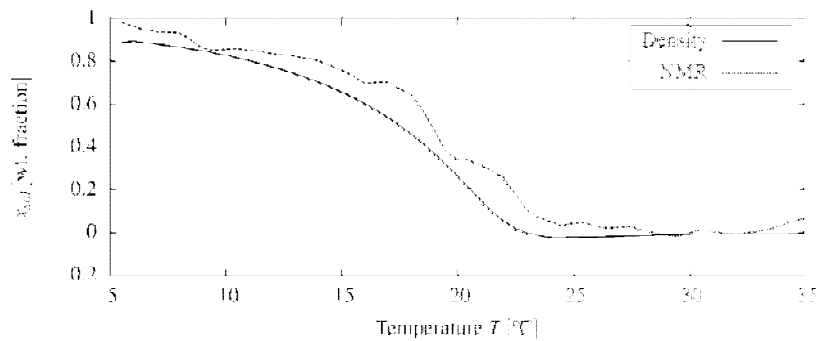


Fig. 7. Estimated solid content from experiments.

The resulting curve for solid content as function of temperature illustrates the behaviour of the PCS during slow temperature changes. If thermodynamic equilibrium cannot be assured, the procedures and data presented here could still be used for a comparison. Depending on the actual application, Fig. 7

can be used to spot and quantify supercooling effects. In theory, ultrasonic technique is suitable to follow phase changes. However, sound scattering occurs and needs to be accounted for. Fraunhofer UM-SICHT conducts ongoing research in the field of phase change slurries. The next steps that will be taken include a verification of the start and end of the phase transition by extending the temperature range in both directions. Additionally, the single-phase volume expansion of paraffin as a function of temperature was not investigated yet.

## 6. Acknowledgement

The authors thank the German Federal Ministry of Economics and Technology for funding the project “EnEff: Emulsionen aus Paraffinen und Wasser für Anwendungen in Versorgungssystemen der Gebäudetechnik” (FKZ 0327471A).

## References

- [1] H. Inaba, New challenge in advanced thermal energy transportation using functionally thermal fluids, *International Journal of Thermal Sciences*, 39 (2000) 991–1003.
- [2] B. Chen, X. Wang, Y. Zhang, H. Xu, R. Yang, Experimental research on laminar flow performance of phase change emulsion, *Applied Thermal Engineering*, 26 (2006) 1238–1245.
- [3] V. Langlois, J. Laurent, X. Jia, W. Gautherin, L. Fournaison, A. Delahaye, L. Royon, Determination of Particle Concentration in a Slurry System by Ultrasonic Technique. *Proceedings of the 8th IIR Conference on Phase Change Materials and Slurries for Refrigeration and Air Conditioning*, 2009.
- [4] Å. Melinder, E. Granryd, Using property values of aqueous solutions and ice to estimate ice concentrations and enthalpies of ice slurries, *International Journal of Refrigeration*, 28 (2005) 13–19.
- [5] L. Klintberg, M. Karlsson, L. Stenmark, J.-A. Schweitz, G. Thornell, A large stroke, high force paraffin phase transition actuator, *Sensors and Actuators A: Physical*, 96 (2002), 189–195.
- [6] M.H. Levitt, (2008). *Spin Dynamics — Basics of Nuclear Magnetic Resonance*, 2nd edition. John Wiley & Sons Ltd, Chichester.
- [7] J.D.N. Cheeke. (2002). *Fundamentals and Applications of Ultrasonic Waves*, CRC Press, Boca Raton.
- [8] W. Schaaffs, Alterations of sound velocity and density with substitution changes, *SpringerMaterials — The Landolt-Börnstein Database*, Volume 5 (1967) 40–44.
- [9] H. Raich, P. Blumler, Design and construction of a dipolar Halbach array with a homogeneous field from identical bar magnets: NMR Mandhalas, *Concepts in Magnetic Resonance Part B: Magnetic Resonance Engineering*, 23B (2004) 16–25.
- [10] W. Wagner, A. Pruss, The IAPWS Formulation 1995 for the Thermodynamic Properties of Ordinary Water Substance for General and Scientific Use, *Journal of Physical and Chemical Reference Data*, 31 (2002) 387–535.
- [11] R.R. Reddy, A. Venkateswarlu, K.N. Reddy, K.R. Gopal, On the behaviour of thermo-acoustic parameters in different liquids, *Journal of Molecular Liquids*, 126 (2006), 9–13.
- [12] J.P.M. Trusler, (1991). *Physical Acoustics and Metrology of Fluids*, Taylor & Francis Group, New York.
- [13] M.J.W. Povey, (1997). *Ultrasonic Techniques for Fluids Characterization*, Academic Press, San Diego.